Effect of target inelastic channels in positronium-hydrogen scattering

Arindam Basu,[1] Prabal K. Sinha,[2] and A. S. Ghosh[1]
[1]*Department of Theoretical Physics, Indian Association for the Cultivation of Science, Jadavpur, Calcutta-700032, West Bengal, India*
[2]*Department of Physics, Bangabasi College, 19, Rajkumar Chakraborty Sarani, Calcutta-700009, West Bengal, India*
(Received 25 February 2000; published 1 December 2000)

Projectile elastic close-coupling method is employed to investigate the positronium-hydrogen scattering using different basis sets to find the rate of convergence with added eigenstates and pseudostates. We report *s*-, *p*-, and *d*- wave phase shifts below the first positronium excitation threshold and also integrated elastic and excitation cross sections along with the corresponding Born-Oppenheimer results up to the incident positronium energy 200 eV. The present pseudostate singlet and triplet *s*-wave phase shifts are in good agreement with those of Drachman and Houston [R. J. Drachman and S. K. Houston, Phys. Rev. A **12**, 885 (1975)]; [R. J. Drachman, *ibid.* **19**, 1900 (1979)] and 22-state target elastic pseudostate close-coupling predictions of Campbell *et al.* [C. P. Campbell *et al.*, Phys. Rev. Lett. **80**, 5097 (1998)]. The effect of the inelastic channels of the target atom on the elastic one at low energies is found to be significant in studying positronium-atom scattering.

DOI: 10.1103/PhysRevA.63.012502 PACS number(s): 36.10.Dr, 34.50.−s

I. INTRODUCTION

The positronium (Ps) atom is an exotic atom and has its own characteristics. The Ps atom is available both in spin triplet (ortho, *o*-) and spin singlet (para, *p*-) states. *o*-Ps annihilates into three photons and *p*-Ps into two photons. The lifetime of *o*-Ps is 10^3-fold longer than that of *p*-Ps. Consequently, the *o*-Ps ($1s$ state), which is sufficiently long-lived, is used as a laboratory projectile. Now a monoenergetic energy tunable beam is available and it is possible to perform scattering experiments with an *o*-Ps atom [1]. However, it is now only possible to measure the total cross section for scattering of Ps off atomic and molecular targets (H_2, He, Ar, and O_2) [2–5]. We consider here the scattering of *o*-Ps ($1s$) with the ground state of a hydrogen (H) atom. Theoretically, Ps-atom scattering is much more difficult than the corresponding electron or positron-atom scattering. This is due to the fact that both Ps and H atoms have internal degrees of freedom [6,7]. An added complication is the fact that it is a four-body problem. Because of the coincidence of the mass and the charge centers, for the process in which the initial and final states of Ps states have the same parity, the direct Born-scattering amplitude (FBA) vanishes regardless of the fact that the parity of the initial and final target states may differ. The importance of this system was first realized by Massey and Mohr [8], who evaluated the FBA using only electron exchange interaction. Fraser [9] and Fraser and Hara [10] calculated the Ps-H scattering for the first time using the static exchange model. Drachman and Houston (DH) [11,12] have provided realistic estimates of the *s*-wave scattering using a variational method. In the S-wave, phase shifts DH have predicted resonance in the singlet scattering due to the fact that positron orbits around the H^- ion. Recently, Ray and Ghosh [13,14] have estimated scattering parameters over a wider energy range using the static exchange model. Sinha *et al.* [15] have employed target elastic three-state $[\mathrm{Ps}(1s,2s,2p),\mathrm{H}(1s)]$ close-coupling approximation (CCA), where the H atom always remains in the ground state, to investigate the system. Ray and Ghosh [16] have investigated the system using projectile elastic three-state $[\mathrm{Ps}(1s),\mathrm{H}(1s,2s,2p)]$ CCA where the Ps atom always remains in the ground state. It has been found by them that the effect of the excitation of the target atom on the elastic scattering is appreciable. The most elaborate calculation of the Ps-H scattering in the framework of target elastic CCA has been carried out by the Belfast group [17] in which they have retained 22 states out of which the first three are eigenstates. Their results are in good agreement with those of DH. They have concluded that the dominating contribution to the cross section is due to the inelastic channels of the Ps atom. Moreover, they have also obtained *s*-wave resonances, though at a slightly different energy as had been predicted by DH. Biswas and Adhikari [18] have performed a coupled-state calculation for the same system in which electron exchange between the two atoms is represented by a model nonlocal tuned exchange potential. They have predicted the existence of resonances in which the positron orbits the H^- ion. However, their cross sections differ appreciably from the other existing theoretical predictions. Most recently, Sinha, Basu, and Ghosh [19] have performed a six-state close-coupling calculation in which the lowest three eigenstates of each atom are retained. This calculation takes the effect of the van der Waals force, which is considered to be important in the atom-atom scattering. We hasten to add that this model has been used by Sinha and Ghosh [7], neglecting electron exchange.

We investigate in this paper $\mathrm{Ps}(1s)+\mathrm{H}(1s)$ scattering using the projectile elastic close-coupling method as done by Ray and Ghosh [16]. Here we employed different basis sets to find the relative importance of each state of the target atom. Moreover, we include the effect of higher excited states of the H atom and continuum via pseudostates [20,21]. It has been assumed by McAlinden and co-workers [6,17] that in Ps-atom scattering, the Ps excitation channels are the dominant processes in predicting reliable estimates for the elastic cross sections at low energies (below 10 eV) and the inelastic channels of the target H atom are not expected to contribute appreciably below 10 eV. Our motivation of this

paper is to find the role played by the inelastic channels of the H atom in Ps-H scattering.

In Sec. II, we briefly describe the theoretical model as employed by us. In Sec. III, we present the results up to 200 eV for scattering parameters using different basis sets and compare them with the existing theoretical results. In conclusion, in Sec. IV we explain the reason for the choice of the basis sets and discuss merits of different models.

II. THEORY

We briefly describe the theoretical model employed here in order to make the article self-consistent. The total wave function for the system of a positronium and a hydrogen atom should be antisymmetric and may be written as

$$\Psi^{\pm}(\vec{r}_p,\vec{r}_1,\vec{r}_2)=A\sum_{nv}\Phi_n(\vec{r}_2)\,\eta_v(\vec{\rho}_1)F^{\pm}_{nv}(R_1), \tag{1}$$

where $\vec{R}_i=\frac{1}{2}(\vec{r}_p+\vec{r}_i)$ and $\vec{\rho}_i=\vec{r}_p-\vec{r}_i$; $i=1,2$.

Here, $\vec{r}_i$ are the position vectors of the electrons with respect to the proton and $\vec{r}_p$ is that of the positron. A is the antisymmetrizing operator and is given by $A=1\pm P_{12}$, where P_{12} is the exchange operator.

The total Hamiltonian of the system in the initial channel is given by

$$H=-\tfrac{1}{4}\vec{\nabla}^2_{R_1}+H_{p_3}(\vec{\rho}_1)+H_H(\vec{r}_2)+V_{\rm int}(\vec{r}_p,\vec{r}_1,\vec{r}_2), \tag{2}$$

where $V_{\rm int}(\vec{r}_p,\vec{r}_1,\vec{r}_2)$ is the interaction potential and is given by

$$V_{\rm int}(\vec{r}_p,\vec{r}_1,\vec{r}_2)=\frac{1}{r_p}-\frac{1}{r_2}-\frac{1}{|\vec{r}_p-\vec{r}_1|}+\frac{1}{|\vec{r}_1-\vec{r}_2|}. \tag{3}$$

Here, H_{Ps} and H_H are the Hamiltonians describing the bound Ps and H atoms, respectively. The total wave function must satisfy the Schrödinger equation for the system,

$$H\Psi^{\pm}(\vec{r}_p,\vec{r}_1,\vec{r}_2)=E\Psi^{\pm}(\vec{r}_p,\vec{r}_1,\vec{r}_2). \tag{4}$$

The wave functions of the hydrogen and positronium atoms satisfy the following Schrödinger equations:

$$H_{\rm H}(\vec{r}_2)\Phi_n(\vec{r}_2)=\varepsilon^{\rm H}_n\vec{\Phi}_n(\vec{r}_2) \tag{5}$$

and

$$H_{\rm Ps}(\vec{\rho}_1)\,\eta_v(\vec{\rho}_1)=\varepsilon^{\rm Ps}_v\eta_v(\vec{\rho}_1), \tag{6}$$

where $\varepsilon^{\rm H}_n$ and $\varepsilon^{\rm Ps}_v$ are the binding of the hydrogen and positronium atoms, respectively.

The exact coupled integral equation in three dimensions for the transition amplitude for the H and Ps atoms in the momentum space may be expressed as [7]

$$\langle K'n'v'|Y^{\pm}|Knv\rangle=\langle K'n'v'|B^{\pm}|Knv\rangle+\sum_{n''}\sum_{v''}\int d\vec{k}''\times\frac{\langle K'n'v'|B^{\pm}|K''n''v''\rangle\langle K''n''v''|Y^{\pm}|Knv\rangle}{E-E''+i\varepsilon}, \tag{7}$$

where

$$\langle K'n'v'|Y^{\pm}|Knv\rangle=\langle K'n'v'|Y_{11}|Knv\rangle\pm\langle K'n'v'|Y_{21}|Knv\rangle.$$

Here, the transition matrix element of Y_{11} stands for the direct channel and the matrix element Y_{21} is that for the exchange channel.

A similar expression for the matrix element $B^{\pm}$ holds good. The transition matrix element for $B^{\pm}$ gives the first Born and Born-Oppenheimer amplitudes.

Assuming the delta function normalization, one can obtain the coupled integral equation for the scattering amplitude as follows:

$$f^{+}_{n'v',nv}(\vec{K}',\vec{K})=f^{B\pm}_{n'v',nv}(\vec{K}',\vec{K})-\frac{1}{2\pi^2}\sum_{n''v''}\int d\vec{K}''\times\frac{f^{B\pm}_{n',v',n'',v''}(\vec{K}',\vec{K}'')f^{\pm}_{n''v'',nv}(\vec{K}'',\vec{K})}{K^2_{n''v''}-K''^2+i\varepsilon}. \tag{8}$$

In the present calculations, we assume that the positronium atom always remains in the ground state. We term this model as projectile elastic close-coupling approximation (CCA).

The scattering amplitude $f^{\pm}$ can be expanded as

$$f^{\pm}_{n'v',nv}(\vec{K}',\vec{K})=\frac{1}{\sqrt{KK'}}\sum_{JMLM_LL'M'_Llml'm'}\begin{pmatrix}L' & l' & J\\ M'_L & m' & M\end{pmatrix}\times Y^{*}_{L'M'_L}(\hat{K}')T^{J\pm}(\tau'\vec{K}',\tau\vec{K})\times\begin{pmatrix}L & l & J\\ M_L & m & M\end{pmatrix}Y_{LM_L}(\vec{K}). \tag{9}$$

A similar expression for $f^{B\pm}$ can also be written as

$$f^{B\pm}_{n'v',nv}(\vec{K}',\vec{K})=\frac{1}{\sqrt{KK'}}\sum_{JMLM_LL'M'_Llm'm'}\begin{pmatrix}L' & l' & J\\ M'_L & m' & M\end{pmatrix}Y^{*}_{L'M'_L}(\hat{K}')\times B^{J\pm}(\tau'\vec{K}';\tau\vec{K})\begin{pmatrix}L & l & J\\ M_L & m & M\end{pmatrix}Y_{LM_L}(\hat{K}). \tag{10}$$

Here, l is the angular momentum of the initial target atom. L is the angular momentum of the moving Ps atom with projection M_L. L combines with l to give the good quantum

TABLE I. *s*-wave phase shifts, scattering length (a) and range parameter (r^0) at selected energies for the different models. K_i is the momentum of the incident positronium atom.

	PE results		TE results			
K_i^2 (a.u.)	$N=3$ eigen	$N=4$ eigen	$N=3$ pseudo	9 ST pseudo (McAlinden and co-workers)	22 ST pseudo (McAlinden and co-workers)	DH variational
			(a) Singlet scattering			
0.1639	1.38	1.41	1.47	1.44	1.50	1.52
0.2478	1.15	1.18	1.26	1.22	1.28	1.27
0.3975	0.90	0.93	0.98	0.96	1.03	1.00
0.5588	0.72	0.74	0.78	0.81	0.89	0.81
a	5.84	5.64	5.22	5.51	5.20	4.5
r_0	2.91	2.83	2.74	2.74	2.52	2.2
			(b) Triplet scattering			
0.0651	−0.611	−0.610	−0.603	−0.611	−0.610	−0.591
0.0878	−0.700	−0.698	−0.689	−0.704	−0.702	−0.6845
0.2315	−1.089	−1.088	−1.084	−1.091	−1.086	−1.051
0.2898	−1.188	−1.186	−1.182	−1.199	−1.191	−1.161
0.5064	−1.487	−1.486	−1.482	−1.493	−1.486	−1.445
a	2.45	2.44	2.41	2.45	2.45	2.36
r_0	1.36	1.35	1.32	1.33	1.32	1.31

number J with projection M. All these quantities are referred to the initial channel. The primed quantities are for the final channel.

By proper algebraic manipulation of the three equations (8), (9), and (10), T's and B's, the resulting one-dimensional coupled inhomogeneous integral equation after the partial wave analysis takes the form

$$T^{J\pm}(\tau'\vec{K}';\tau\vec{K}) = B^{J\pm}(\tau'\vec{K}',\tau\vec{K}) - \frac{1}{2\pi^2}\sum_{\tau''}\int dK''K''^2 \times \frac{B^{J\pm}(\tau'\vec{K}',\tau''\vec{K}'')T^{J\pm}(\tau''\vec{K}'',\tau\vec{K})}{K^2_{n''v''} - K''^2 + i\varepsilon}, \quad (11)$$

where $\tau \equiv (n,l,L)$.

To solve this integral equation we require the values of $B^{J\pm}$ for each transition. The first Born direct and exchange amplitude are given, respectively, as follows:

$$f^B = -\frac{\mu}{2\pi}\int e^{-i\vec{k}'\cdot\vec{R}_1}\eta_{1s}(\vec{\rho}_1)\Phi_{n'l'm'}(\vec{r}_2)V_{\rm int} \times e^{i\vec{k}\cdot R_1}\eta_{1s}(\vec{\rho}_1)\Phi_{\rm nlm}(\vec{r}_2)d\vec{R}_1 d\vec{\rho}_1 d\vec{r}_2, \quad (12)$$

$$g^B = -\frac{\mu}{2\pi}\int e^{-i\vec{k}'\cdot\vec{R}_2}\eta_{1s}(\vec{\rho}_2)\Phi_{n'l'm'}(\vec{r}_1) \times [H-E]e^{i\vec{k}\cdot\vec{R}_1}\eta_{1s}(\vec{\rho}_1)\Phi_{\rm nlm}(\vec{r}_2)d\vec{r}_p d\vec{r}_1 d\vec{r}_2. \quad (13)$$

Evaluation of f^B is straightforward and in Appendix A. We evaluate exchange amplitude for the transition H($n00 \rightarrow n'l'm'$).

The scattering parameters are calculated by standard relation. In the present calculations we use the following basis sets: (a) H(1*s*,2*s*,3*s*,2*p*,3*p*,3*d*)+Ps(1*s*), (b) H(1*s*,2*s*,3*s*,4*s*,2*p*,3*p*,4*p*,3*d*,4*d*)+Ps(1*s*), (c) H(1*s*,2*s*,2*p*, $3\overline{s},3\overline{p},3\overline{d}$)+Ps(1*s*). In the basis set (c), we use three pseudostates $3\overline{s}$, $3\overline{p}$, and $3\overline{d}$. We take the $3\overline{s}$, $3\overline{p}$ from Burke *et al.* [21] and $3\overline{d}$ from Damburg and Karule [20]. Our motive of including simple pseudostates is to estimate the effect of higher excited states and of continuum of the target atom. Use of some more accurate pseudostates prepared specially for this system may give more accurate results.

III. RESULTS AND DISCUSSIONS

The one-dimensional coupled integral equation (11) is solved numerically using the matrix inversion method. Numerical code as employed by Ray and Ghosh [16] and Sinha *et al.* [15] is extended and used. As a check of our program, three-state target elastic (TE) and projectile elastic (PE) results of Sinha *et al.* and Ray and Ghosh are reproduced. We emphasize that inclusion of *d* states of the H atom, either eigen or pseudo, has a marginal effect on the elastic scattering parameters, but influences the inelastic channels.

The *s*-wave phase shifts below the Ps excitation threshold are given in Table I. This provides validity and accuracy of our model in predicting scattering parameters. Table I contains *s*-wave singlet (a) and triplet (b) phase shifts of our three projectile elastic models. This table also includes the corresponding scattering phase shifts using target elastic CCA (9 ST and 22 ST) of McAlinden and co-workers at

TABLE II. *p*-wave elastic phase shifts (radians).

K_i (a.u.)	Eigenstates				Pseudostates
	$N=1$	$N=2$	$N=3$	$N=4$	$N=3$
			(a) Singlet scattering		
0.1	7.98(−3)	9.15(−3)	9.32(−3)	9.37(−2)	9.59(−2)
0.2	6.14(−2)	7.16(−2)	7.29(−2)	7.34(−2)	7.58(−2)
0.3	1.88(−1)	2.21(−1)	2.25(−1)	2.26(−1)	2.36(−1)
0.4	3.94(−1)	4.18(−1)	4.25(−1)	4.28(−1)	4.51(−1)
0.5	4.77(−1)	5.69(−1)	5.80(−1)	5.83(−1)	6.15(−1)
0.6	5.36(−1)	6.36(−1)	6.50(−1)	6.54(−1)	6.87(−1)
0.7	5.38(−1)	6.41(−1)	6.57(−1)	6.62(−1)	6.93(−1)
0.8	5.08(−1)	6.11(−1)	6.29(−1)	6.35(−1)	6.63(−1)
			(b) Triplet scattering		
0.1	−5.03(−3)	−4.71(−3)	−4.66(−3)	−4.65(−3)	−4.62(−3)
0.2	−3.52(−2)	−3.31(−2)	−3.27(−2)	−3.27(−2)	−3.25(−2)
0.3	−9.80(−2)	−9.24(−2)	−9.18(−2)	−9.16(−2)	−9.12(−2)
0.4	−1.86(−1)	−1.76(−1)	−1.75(−1)	−1.75(−1)	−1.74(−1)
0.5	−2.87(−1)	−2.72(−1)	−2.71(−1)	−2.70(−1)	−2.69(−1)
0.6	−3.90(−1)	−3.70(−1)	−3.68(−1)	−3.67(−1)	−3.66(−1)
0.7	−4.88(−1)	−4.61(−1)	−4.58(−1)	−4.58(−1)	−4.58(−1)
0.8	−5.74(−1)	−5.40(−1)	−5.36(−1)	−5.35(−1)	−5.36(−1)

available energies. The corresponding phase shifts of Drachman and Houston (DH) are also cited for comparison. We hasten to add that the scattering length and effective range of all the theoretical models are also shown. From the table it is apparent that present PE *s*-wave singlet phase shifts monotonically increase with addition of eigenstates or addition of pseudostates as expected at the energies considered. In the case of triplet scattering, the trend is found to be similar although marginal. This feature has also been noticed by McAlinden and co-workers as well as by Sinha *et al.* (ST). Now we compare our present results with those of TE CCA results of McAlinden and co-workers and the variational predictions of DH that are considered as realistic ones. Present $N=4$ eigenstate singlet phase shifts are definitely an improvement over the $N=3$ eigenstate results, when compared with variational predictions of DH $N=3$ pseudostate singlet phase shifts are a further improvement over the eigenstate results. $N=4$ eigenstate PE results are very close to the 9 ST TE results of McAlinden and co-workers whereas $N=3$ pseudostate PE results are close to 22 ST TE results of McAlinden and co-workers. Here we have used very simple pseudostates available in the literature [20,21]. Use of more suitable pseudostates of the H atom for this particular system may improve the results appreciably. Our scattering length and effective range are also found to improve with addition of eigenstates or pseudostates. The triplet scattering phase shifts do not vary appreciably with different basis sets at the energies considered here. These have also been noticed by McAlinden and co-workers. However, our $N=3$ pseudostate PE results are in the closest agreement with the corresponding predictions of DH. The present *s*-wave phase shifts indicate that excitation of the H atom is also very important in investigating $\mathrm{Ps}(1s)+\mathrm{H}(1s)$ scattering.

In Table II, we present our *p*-wave singlet (a) and triplet (b) phase shifts. At low energies the magnitude of phase shifts, either singlet or triplet, are very small. With the increase of energy, phase shifts of different models change as expected. As there are no existing P-wave phase shifts, we cannot compare our results. D-wave singlet and triplet phase shifts are tabulated in Table III(a) and III(b), respectively. In the case of singlet phase shifts, the results increase with the addition of states, results of the pseudostate being the highest. Similarly, triplet phase shifts also increase with the addition of states and the pseudostate results being the highest. Thus we see inclusion of higher excited states and continuum influences the low-energy scattering parameters. *p*-wave and *d*-wave phase shifts are tabulated as a future reference.

Figure 1 displays the integrated elastic cross sections up to the incident Ps energy 5 eV. In the inset of Fig. 1, the elastic cross sections for the different sets below 1 eV are shown. With the increase of eigenstates or pseudostates in the expansion basis, elastic cross sections decrease significantly. $N=3$ pseudostate results decrease by about 30% from the static exchange results ($N=1$ cross section is $58\pi a_0^2$ and $N=3$ pseudostate cross section reduces to $40\pi a_0^2$) at the lowest incident energy considered. It may be mentioned that the results of Biswas and Adhikari [18] are about 40–45 % less than the present pseudostate results at the lowest energy, but it differs from other theoretical findings. With the increase in energy, the difference between the different models decreases (Table IV). At about 80 eV, the elastic cross section using different basis sets coalesce among themselves.

Table V presents $\mathrm{H}(1s\text{-}2s)$ PE excitation cross sections using different models along with the Born-Oppenheimer (BO) cross sections. Here, we recalculate PE $N=2$ state calculations as performed by Ray and Ghosh [16]. The present

TABLE III. *d*-wave elastic phase shifts (radians).

K_i (a.u.)	Eigenstates $N=1$	$N=2$	$N=3$	$N=4$	Pseudostates $N=3$
			(a) Singlet scattering		
0.1	3.18(−5)	3.28(−5)	3.55(−5)	3.58(−5)	3.59(−5)
0.2	9.17(−4)	9.44(−4)	1.01(−3)	1.11(−3)	1.16(−3)
0.3	5.87(−3)	6.06(−3)	6.45(−3)	6.51(−3)	6.53(−3)
0.4	1.97(−2)	2.04(−2)	2.15(−2)	2.16(−2)	2.17(−2)
0.5	4.54(−2)	4.69(−2)	4.90(−2)	4.96(−2)	4.98(−2)
0.6	8.09(−2)	8.37(−2)	8.70(−2)	8.85(−2)	8.90(−2)
0.7	1.19(−1)	1.24(−1)	1.28(−1)	1.29(−1)	1.31(−1)
0.8	1.52(−1)	1.58(−1)	1.64(−1)	1.65(−1)	1.67(−1)
			(b) Triplet scattering		
0.1	−3.00(−5)	−2.81(−5)	−2.60(−5)	−2.58(−5)	−2.58(−5)
0.2	−8.56(−4)	−8.01(−4)	−7.45(−4)	−7.44(−4)	−7.43(−4)
0.3	−5.37(−3)	−5.02(−3)	−4.73(−3)	−4.69(−3)	−4.68(−3)
0.4	−1.76(−2)	−1.64(−2)	−1.56(−2)	−1.55(−2)	−1.54(−2)
0.5	−3.95(−2)	−3.70(−2)	−3.55(−2)	−3.52(−2)	−3.51(−2)
0.6	−7.03(−2)	−6.55(−2)	−6.33(−2)	−6.28(−2)	−6.22(−2)
0.7	−1.06(−1)	−9.85(−2)	−9.56(−2)	−9.48(−2)	−9.46(−2)
0.8	−1.42(−1)	−1.32(−1)	−1.28(−1)	−1.27(−1)	−1.26(−1)

$N=2$ state results differ slightly from Ray and Ghosh as the presents coupled integral equation is solved using two large sets of Gaussian points ($0-2K_n$ and $2K_n-\infty$). However, present elastic results do not differ from those of Ray and Ghosh. Table V indicates that the effect of higher excited states influences the H(1*s*-2*s*) cross sections. This feature has also been noticed in the H(1*s*-3*s*) PE excitation cross section (Table VI). We also estimate the H(1*s*-4*s*) PE results (Table VI) for future reference. In all the cases, BO cross sections coalesce with the CCA predictions at energies 80 eV and above. In absence of any other theoretical data we

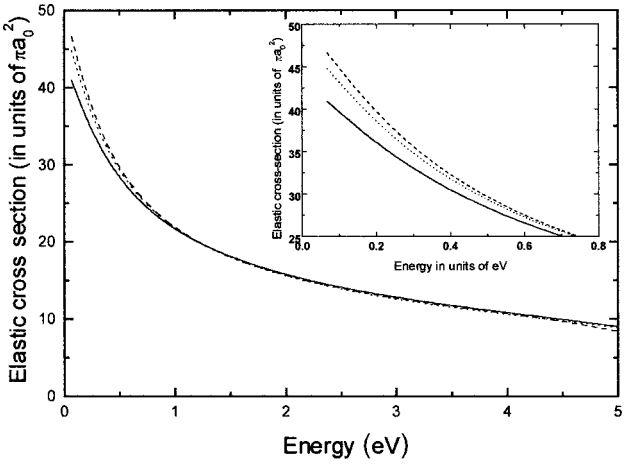

FIG. 1. Elastic cross sections up to 5 eV of different basis sets. Dashed curve represents $N=3$ eigenstate results, dotted curve represents $N=4$ eigenstate results and the solid curve represents $N=3$ pseudostate results. In the inset, elastic cross sections up to 0.8 eV for the different basis sets are shown. The curves depict the basis sets as stated above.

TABLE IV. Integrated elastic, $H(1s)+Ps(1s)\rightarrow H(1s)+Ps(1s)$, CCA cross section (units of πa_0^2). The figure in parentheses indicates power of 10.

Energy (eV)	$N=3$ eigen	$N=4$ eigen	$N=3$ pseudo
0.068	46.53	44.77	40.94
0.272	35.47	34.81	33.17
0.612	26.34	26.17	25.68
1.088	20.48	20.45	20.44
1.700	16.69	16.63	16.80
2.448	13.98	13.86	14.10
3.332	11.86	11.68	11.98
4.352	10.11	9.87	10.21
5.508	8.59	8.31	8.67
6.000	8.04	7.75	8.10
6.800	7.23	6.91	7.27
10.0	4.30	3.98	4.25
15.0	2.06	1.43	1.28
20.0	1.04	7.19(−1)	9.37(−1)
25.0	5.51(−1)	4.31(−1)	5.86(−1)
30.0	3.39(−1)	1.73(−1)	3.57(−1)
40.0	2.23(−2)	5.30(−2)	1.67(−1)
50.0	3.19(−2)	3.01(−2)	1.08(−1)
60.0	3.53(−2)	3.69(−2)	3.09(−2)
80.0	2.98(−2)	3.03(−2)	2.86(−2)
100.0	2.18(−2)	2.17(−2)	2.16(−2)
150.0	9.64(−3)	9.63(−3)	9.62(−3)
200.0	4.76(−3)	4.76(−3)	4.75(−3)

TABLE V. H($1s$-$2s$) excitation cross section (πa_0^2). Ps always remains in $1s$ state. The figure in parentheses indicates power of 10.

Energy (eV)	B-O	CCA $N=2$	CCA $N=3$	CCA $N=4$
15.0	4.11(−1)	3.06(−1)	2.71(−1)	1.50(−1)
20.0	2.34(−1)	2.30(−1)	2.29(−1)	2.32(−1)
25.0	1.25(−1)	1.39(−1)	1.49(−1)	1.93(−1)
30.0	6.57(−2)	8.50(−2)	1.06(−1)	1.07(−1)
40.0	1.79(−2)	1.34(−2)	1.49(−2)	2.27(−2)
50.0	4.92(−3)	4.21(−3)	4.19(−3)	6.20(−3)
60.0	1.48(−3)	1.42(−3)	1.42(−3)	1.63(−3)
80.0	4.57(−4)	4.86(−4)	4.88(−4)	4.56(−4)
100.0	4.32(−4)	4.46(−4)	4.47(−4)	4.37(−4)
150.0	2.93(−4)	2.94(−4)	2.94(−4)	2.94(−4)
200.0	1.64(−4)	1.64(−4)	1.64(−4)	1.64(−4)

cannot compare our coupled state results.

Now we discuss H($1s$-Np) PE excitation cross sections that we have obtained using different models. Table VII presents three sets of H($1s$-$2p$) CCA results along with the BO results. Below 30 eV, with the addition of eigenstates $2p$ cross sections decrease, $N=4$ state results being the lowest. Different sets of results indicate the cross section varies with added eigenstates. However, as in the case of H($1s$-Ns) excitation ($N\neq 1$) transitions, the magnitude of the cross section is low. In the case of H($1s$-$3p$) transition (Table VIII), a similar pattern to H($1s$-$2p$) has been noticed. However, the influence of higher excited states on the cross section is not as significant as in the case of H($1s$-$2p$). This may be due to the fact that we have neglected higher ($N>4$)p states in the calculations. In all the cases, BO results are found to be in close agreement with CCA results at about 80 eV. Table VIII also contains H($1s$-$4p$) results along with BO. At low energies as in the case of other transitions, BO results differ from CCA predictions appreciably. The BO results for H($1s$-$4p$) excitation cross sections coalesce with those of CCA at 150 eV.

Table IX presents the H($1s$-$3d$) and H($1s$-$4d$) CCA results along with the corresponding BO cross sections. H($1s$-$3d$) results have the same pattern as H($1s$-Np) results. $N=3$ and $N=4$CCA predictions for the H($1s$-$3d$) transition coalesce at the incident energy at 80 eV and above. In the present case, BO results differ significantly from both sets of CCA results. With the increasing energy, the difference between the BO and CCA results decreases. However, at the highest energy considered (200 eV) the BO result does not coalesce with either of the CCA predictions. In the case of H($1s$-$4d$) excitation cross sections the present CCA results differ throughout the energy range from the corresponding BO cross section.

IV. CONCLUSION

In this paper, we investigated o-Ps($1s$) + H($1s$) scattering using projectile elastic close-coupling approximation (PE CCA). Three different basis sets, (a) Ps($1s$) + H($1s$,$2s$,$3s$,$2p$,$3p$,$3d$), (b) Ps($1s$) + H($1s$,$2s$,$3s$,$4s$,$2p$, $3p$,$4p$,$3d$,$4d$), (c) Ps($1s$) + H($1s$,$2s$,$2p$,$3\bar{s}$,$3\bar{p}$,$3\bar{d}$), are employed to find the relative importance of higher excited states and continuum in predicting the scattering parameters of the elastic channel and of lower excitation channels. We report the s-, p-, and d-wave singlet and triplet phase shifts for incident energies below the Ps-excitation threshold. It has been found that the higher excited states of the target H atom influences the low-energy phase shifts appreciably. The rate of convergence of the elastic phase shifts decreases with added eigenstates in the expansion scheme. The effect of the continuum on the elastic channel is also very prominent. We compare the present s-wave phase shifts at selected energies with the corresponding theoretical predictions of DH and the 9-ST and the 22-ST target elastic pseudostate CCA of the Belfast Group (BG). The present $N=4$ CCA results are in fair agreement with the corresponding 9-ST results of BG whereas our pseudostate CCA results agree well with the 22-ST predictions of BG. The present pseudostate predictions tally well with the variational calculations of DH. The

TABLE VI. H($1s$-$3s$) and H($1s$-$4s$) excitation cross sections (πa_0^2). Ps always remains in $1s$ states. The figure in parentheses indicates power of 10.

Energy (eV)	H($1s$-$3s$) B-O	H($1s$-$3s$) CCA $N=3$	H($1s$-$3s$) CCA $N=4$	H($1s$-$4s$) B-O	H($1s$-$4s$) CCA $N=4$
15.0	1.04(−1)	5.55(−2)	6.35(−2)	3.94(−2)	2.27(−2)
20.0	7.05(−2)	6.22(−2)	6.86(−2)	2.94(−2)	2.75(−2)
25.0	4.12(−2)	4.20(−2)	5.47(−2)	1.78(−2)	2.30(−2)
30.0	2.31(−2)	2.31(−2)	3.11(−2)	1.02(−2)	1.34(−2)
40.0	6.92(−3)	6.43(−3)	7.72(−3)	3.16(−3)	3.49(−3)
50.0	2.06(−3)	2.00(−3)	2.14(−3)	9.64(−4)	1.00(−3)
60.0	6.35(−4)	6.21(−4)	6.34(−4)	3.02(−4)	3.02(−4)
80.0	1.26(−4)	1.30(−4)	1.29(−4)	5.41(−5)	5.48(−5)
100.0	9.87(−5)	1.02(−4)	1.03(−4)	3.83(−5)	4.00(−5)
150.0	7.13(−5)	7.22(−5)	7.23(−5)	2.81(−5)	2.85(−5)
200.0	4.07(−5)	4.08(−5)	4.09(−5)	1.62(−5)	1.63(−5)

TABLE VII. H($1s$-$2p$) excitation cross sections (πa_0^2). Ps always remains in $1s$ state. The figure in parentheses indicates power of 10.

Energy (eV)	B-O	CCA $N=2$	CCA $N=3$	CCA $N=4$
15.0	3.95(−1)	5.32(−1)	4.82(−1)	3.72(−1)
20.0	1.87(−1)	3.74(−1)	3.68(−1)	2.17(−1)
25.0	8.25(−2)	2.29(−1)	2.26(−1)	1.82(−1)
30.0	4.87(−2)	1.61(−1)	1.63(−1)	1.72(−1)
40.0	3.45(−2)	3.01(−2)	3.12(−2)	5.93(−2)
50.0	2.85(−2)	2.56(−2)	2.53(−2)	2.85(−2)
60.0	2.23(−2)	2.13(−2)	2.12(−2)	2.09(−2)
80.0	1.27(−2)	1.26(−2)	1.26(−2)	1.25(−2)
100.0	7.33(−3)	7.31(−3)	7.31(−3)	7.27(−3)
150.0	2.27(−3)	2.27(−3)	2.27(−3)	2.27(−3)
200.0	9.21(−4)	9.22(−4)	9.22(−4)	9.21(−4)

TABLE VIII. H($1s$-$3p$) and H($1s$-$4p$) excitation cross sections (πa_0^2). Ps always remains in $1s$ states. The figure in parentheses indicates power of 10.

Energy	H($1s$-$3p$)			H($1s$-$4p$)	
(eV)	B-O	CCA $N=3$	CCA $N=4$	B-O	CCA $N=4$
15.0	9.33(−2)	2.96(−1)	1.57(−1)	2.76(−2)	5.66(−2)
20.0	7.11(−2)	1.94(−1)	1.42(−1)	3.03(−2)	6.69(−2)
25.0	3.22(−2)	9.11(−2)	8.85(−2)	1.58(−2)	3.95(−2)
30.0	1.51(−2)	4.55(−2)	5.37(−2)	7.52(−3)	6.77(−3)
40.0	7.36(−3)	6.88(−3)	1.40(−2)	3.21(−3)	3.14(−3)
50.0	6.20(−3)	5.38(−3)	6.40(−3)	2.59(−3)	1.80(−3)
60.0	5.20(−3)	4.89(−3)	4.90(−3)	2.12(−3)	1.87(−3)
80.0	3.22(−3)	3.18(−3)	3.16(−3)	1.19(−3)	1.03(−3)
100.0	1.93(−3)	1.92(−3)	1.91(−3)	6.05(−4)	6.04(−3)
150.0	6.13(−4)	6.13(−4)	6.13(−4)	1.15(−4)	1.15(−3)
200.0	2.50(−4)	2.50(−4)	2.50(−4)	2.63(−5)	2.63(−4)

TABLE IX. H($1s$-$3d$) and H($1s$-$4d$) excitation cross sections (πa_0^2). Ps always remains in $1s$ states. The figure in the parentheses indicates power of 10.

Energy	H($1s$-$3d$)			H($1s$-$4d$)	
(eV)	B-O	CCA $N=3$	CCA $N=4$	B-O	CCA $N=4$
15.0	5.50(−2)	3.26(−1)	1.68(−1)	2.42(−2)	4.80(−1)
20.0	3.79(−2)	2.01(−1)	1.52(−1)	2.21(−2)	5.02(−1)
25.0	1.18(−2)	8.28(−2)	8.43(−2)	8.03(−3)	3.20(−1)
30.0	4.70(−3)	3.13(−2)	4.18(−2)	2.49(−3)	1.82(−1)
40.0	1.11(−2)	1.33(−2)	1.75(−2)	4.50(−3)	4.01(−2)
50.0	1.56(−2)	1.87(−2)	1.91(−2)	7.04(−3)	2.68(−2)
60.0	1.53(−2)	1.88(−2)	1.87(−2)	7.25(−3)	2.48(−2)
80.0	1.07(−2)	1.32(−2)	1.32(−2)	5.30(−3)	1.66(−2)
100.0	6.87(−3)	8.43(−3)	8.42(−3)	3.45(−3)	1.01(−2)
150.0	2.49(−3)	2.99(−3)	2.99(−3)	1.26(−3)	3.27(−3)
200.0	1.11(−3)	1.31(−3)	1.31(−3)	5.64(−4)	1.32(−3)

agreement between our results and those of DH are acceptable. Our *s*-wave triplet phase shifts, like others (DH and BG), do not vary appreciably with added eigenstates. Reported *p*- and *d*-wave phase shifts carry the signature of the added eigenstates. Regarding the angle integrated elastic cross section, it is found that at incident energy 0.01 Ry, the cross section decreases steadily from $58\,\pi a_0^2$ (static exchange model) with the addition of eigen or pseudostates in the expansion basis, the lowest cross section (about $40\,\pi a_0^2$) at this energy is obtained in the present $N=3$ pseudostate calculation, a decrease of about 30% whereas the 22-ST calculation of BG predicts this value to be 46 (as estimated from their figure)—a decrease of about 20%. In the calculation, the simple-minded pseudostates due to Burke *et al.* [21] and Damburg and Karule [20] have been used. Our motivation is not only to get numbers. The pseudostates are used to perceive the effect of the target continuum on the elastic channel. The use of more refined pseudostates specially developed for this system may decrease the elastic cross section further and the singlet phase shifts are expected to undergo modification so as to reduce the differences with estimates of DH. It has been shown by BG that the projectile inelastic channels influence the elastic cross section dominantly. The present calculations show that the target excitations also play an important role in predicting the elastic cross section. It is worthwhile to study the target and projectile excitation processes to revel the dynamics of the system. It is worthwhile to study the effect of target and projectile excitations explicitly on the same footing. This will reveal the dynamics of the system. It is not unwise to mention that for Ps-He scattering below 15 eV, where the 22-ST TE CCA calculation of BG [1] differs from the measured data appreciably, theoretical predictions being higher. 3 ST TE CCA of Sarkar *et al.* [22] also predicts higher values. However, results of Sarkar *et al.* are in good agreement with the measured data at energies above 20 eV and above. Biswas and Adhikari [23] as in the case of H, are in fair agreement with the measured data at low energies. However, their results differ significantly from both Sarkar *et al.* and BG. In Ps-atom scattering below 5.1 eV, the total cross section is nothing but the elastic one. Our study on Ps-H indicates that the low-energy elastic cross section is reduced by about 30% on considering the target excitations in the expansion scheme. Moreover, Sinha *et al.* [19] have found that the cross sections at low energies are reduced further when simultaneous excitations of both the target and the projectile atoms are taken into account. Therefore, we advocate strongly for the study of the Ps-He system using projectile elastic CCA and a full CCA (allowing an internal degree of freedom of both the target and projectile atoms).

ACKNOWLEDGMENTS

The authors are thankful to the Department of Science and Technology, Government of India for the financial support (Grant No. SP/S2/K-31/96). One of us, A.B., is grateful to CSIR, Government of India for financial support (Contract No. 9/80(297)/99-EMR-I).

APPENDIX

The expression for the scattering amplitude of Ps-H scattering for the transition from the initial state $(n00)$ of the H atom having momentum $\vec{K}$ to the final state $(n'l'm')$ of the H atom having momentum $\vec{K}'$ is given here. We hasten to add that the Ps atom remains fixed in its ground state throughout the transition. The direct scattering amplitude for this transition is straightforward.

We provide here the analytical expression for the Born-Oppenheimer amplitude for this transition. The Born-Oppenheimer scattering amplitude is given by

$$g^B = -\frac{\mu}{2\pi}\int e^{-i(1/2)\vec{K}'\cdot(\vec{r}_p+\vec{r}_2)}\eta_{1s}^*(\vec{\rho}_2)\Phi_{n'l'm'}^*(\vec{r}_1) \times (H-E)\,\eta_{1s}(\vec{\rho}_1)\Phi_{ns}(\vec{r}_2)e^{i(1/2)\vec{K}\cdot(\vec{r}_p+\vec{r}_1)}d\vec{r}_p d\vec{r}_1 d\vec{r}_2 . \tag{A1}$$

This expression can be expressed as

$$g^B = -\frac{\mu}{2\pi}\int e^{-i(1/2)\vec{K}'\cdot(\vec{r}_p+\vec{r}_2)}\eta_{1s}^*(\vec{\rho}_2)\Phi_{n'l'm'}^*(\vec{r}) \times\{V_{\rm int}+(E''-E)\}\,\eta_{1s}(\vec{\rho}_1)\Phi_{ns}(\vec{r}_2)e^{i(1/2)\vec{K}\cdot(\vec{r}_p+\vec{r}_1)} \times d\vec{r}_p d\vec{r}_1 d\vec{r}_2 . \tag{A2}$$

Please note, on the physical energy shell, $(E''-E)=0$. The term $(E''-E)$ will contribute in the second term of the integral equation (8) on the right-hand side. Therefore, g^B consists of five terms. In performing the calculation, integration of $d\vec{r}_1$ is done after performing the integration over $d\vec{r}_p$ and $d\vec{r}_2$.

The wave function of the H atom in an arbitrary state is given by

$$\Phi_{nlm}(\vec{r}) = \sum_j C(nl;j)\left(-\frac{\partial}{\partial\beta}\right)^{n_j-1-l} re^{-\beta r}Y_{lm}(\hat{r}) \tag{A3}$$

The wave function of the Ps atom in the ground state is given by

$$\eta_{1s}(\vec{\rho}) = \frac{1}{\sqrt{8\pi}}\mathbf{e}^{-\alpha\rho}. \tag{A4}$$

The scattering amplitude involving off the energy shell term $(E''-E)$ is given by

$$g^{B}_{n'l'm',ns}=-\frac{\mu}{2\pi}(E''-E)\int e^{-i(1/2)\vec{K}'\cdot(\vec{r}_p+\vec{r}_2)}\eta^{*}_{1s}(\vec{\rho}_2)\Phi^{*}_{n'l'm'}(\vec{r}_1)\,\eta_{1s}(\vec{\rho}_1)\Phi_{ns}(\vec{r}_2)e^{i(1/2)\vec{K}\cdot(\vec{r}_p+\vec{r}_2)}d\vec{r}_p d\vec{r}_1 d\vec{r}_2. \quad \text{(A5)}$$

Here, μ is the reduced mass of the system and its value is 2.

The final expression after performing the integration is given by

$$\begin{aligned}g^{B}_{n'l'm',ns}(E''-E)=&-i^{l'}2\sqrt{\pi}2^{l'}\Gamma(l'+2)\alpha_i\alpha_f(E''-E)\sum_j C(ns;j)\left(-\frac{\partial}{\partial\beta_i}\right)^{n_j-1}\\&\times\sum_{j'} C(n'l';j')\left(-\frac{\partial}{\partial\beta_f}\right)^{n'_{j'}-1-l'}\beta_i\int_0^1 dy\,y(1-y)\\&\times\int_0^1 dz\,z(1-z)\left(\frac{1}{\mu_1}\frac{\partial}{\partial\mu_1}\right)^2\left(\frac{1}{\mu_2}\frac{\partial}{\partial\mu_2}\right)^2\frac{1}{\mu_2}\frac{\lambda}{(\rho^2+\lambda^2)^{l'+2}}\rho^{l'}Y_{l'm'}(\hat{\rho}),\end{aligned} \quad \text{(A6)}$$

where

$$\mu_1^2=y\alpha_i^2+(1-y)\alpha_f^2+\tfrac{1}{4}y(1-y)Q^2,\quad \vec{Q}=\vec{K}-\vec{K}',\quad \mu_2^2=\mathbf{z}\beta_i^2+(1-z)\mu_1^2+z(1-z)\rho_1^2,$$

$$\vec{\rho}_1=\tfrac{1}{2}\{y\vec{K}-(1+y)\vec{K}'\},\quad \lambda=\mu_2+\beta_f,\quad \vec{\rho}=\tfrac{1}{2}\{(2-y+yz)\vec{K}-(1-y+z+yz)\vec{K}'\}. \quad \text{(A7)}$$

α_i and α_f are the range parameters of the Ps atom in its initial and final states, respectively.

The final expression for the scattering amplitude involving the potential term $1/r_p$ is given by

$$\begin{aligned}g^{B}_{n'l'm',ns}\left(\frac{1}{r_p}\right)=&\,i''2\sqrt{\pi}2^{l'}\Gamma(l'+2)\alpha_i\alpha_f\sum_j C(ns;j)\left(-\frac{\partial}{\partial\beta_i}\right)^{n_j-1}\sum_{j'} C(n'l';j')\left(-\frac{\partial}{\partial\beta_f}\right)^{n'_{j'}-1-l'}\beta_i\int_0^1 dy\,y(1-y)\\&\times\int_0^1 dz\,z\left(\frac{1}{\mu_3}\frac{\partial}{\partial\mu_3}\right)^2\frac{1}{\mu_3}\left(\frac{1}{\mu_4}\frac{\partial}{\partial\mu_4}\right)\frac{1}{\mu_4}\frac{\lambda_1}{(\rho_4^2+\lambda_1^2)^{l'+2}}\rho_4^{l'}Y_{l'm'}(\hat{\rho}_4),\end{aligned} \quad \text{(A8)}$$

where

$$\mu_3^2=y\alpha_f^2+(1-y)\beta_i^2+\tfrac{1}{4}y(1-y)K'^2,\quad \mu_4^2=z\alpha_i^2+(1-z)\mu_1^2+z(1-z)\rho_3^2,\quad \vec{\rho}_3=\tfrac{1}{2}\{\vec{K}-(2-y)\vec{K}'\},$$

$$\lambda_1=\mu_4+\beta_f,\quad \vec{\rho}_4=\tfrac{1}{2}\{(2-z)\vec{K}-(1-z)(2-y)\vec{K}'\}. \quad \text{(A9)}$$

The final expression for the scattering amplitude involving the potential term $1/r_2$ is given by

$$\begin{aligned}g^{B}_{n'l'm',ns}\left(\frac{1}{r_2}\right)=&-i^{l'}2\sqrt{\pi}2^{l'}\Gamma(l'+2)\alpha_i\alpha_f\sum_j C(ns;j)\left(-\frac{\partial}{\partial\beta_i}\right)^{n_j-1}\sum_{j'} C(n'l';j')\left(-\frac{\partial}{\partial\beta_f}\right)^{n'_{j'}-1-l'}\int_0^1 dy\,y(1-y)\\&\times\int_0^1 dz\,z\left(\frac{1}{\mu_1}\frac{\partial}{\partial\mu_1}\right)^2\left(\frac{1}{\mu_5}\frac{\partial}{\partial\mu_5}\right)^2\frac{1}{\mu_5}\frac{\lambda_2}{(\rho_5^2+\lambda_2^2)^{l'+2}}\rho_5^{l'}Y_{l',m'}(\hat{\rho}_5),\end{aligned} \quad \text{(A10)}$$

where

$$\mu_5^2=z\mu_1^2+(1-z)\beta_i^2+z(1-z)\rho_1^2,\quad \lambda_2=\mu_5+\beta_f,\quad \vec{\boldsymbol{\rho}}_5=\tfrac{1}{2}\{(2-yz)\vec{K}-(2-z-yz)\vec{K}'\}. \quad \text{(A11)}$$

The final expression for the scattering amplitude involving the potential term $1/|\vec{r}_p-\vec{r}_1|$, is given by

$$\begin{aligned}g^{B}_{n'l'm',ns}\left(\frac{1}{|\vec{r}_p-\vec{\rho}_1|}\right)=&-i^{l'}2\sqrt{\pi}2^{l'}\Gamma(l'+2)\alpha_f\sum_j C(ns;j)\left(-\frac{\partial}{\partial\beta_i}\right)^{n_j-1}\sum_{j'} C(n'l',j')\left(-\frac{\partial}{\partial\beta_f}\right)^{n'_{j'}-1-l'}\beta_i\int_0^1 dy\,y\\&\times\int_0^1 dz\,z(1-z)\left(\frac{1}{\mu_1}\frac{\partial}{\partial\mu_1}\right)\left(\frac{1}{\mu_6}\frac{\partial}{\partial\mu_6}\right)^2\frac{1}{\mu_6}\frac{\lambda_3}{(\rho_6^2+\lambda_3{}^2)^{l'+2}}\rho_6^{l'}Y_{l'm'}(\hat{\rho}_6),\end{aligned} \quad \text{(A12)}$$

where

$$\mu_6^2 = z\beta_i^2 + (1-z)\mu_1^2 + z(1-z)\rho_2^2, \quad \vec{\rho}_2 = \tfrac{1}{2}\{(1-y)\vec{K} - (2-y)\vec{K}'\},$$

$$\lambda_3 = \mu_6 + \beta_f, \quad \vec{\rho}_6 = \tfrac{1}{2}\{(1-y+z+yz)\vec{K} - (2-y+yz)\vec{K}'\}. \tag{A13}$$

The final expression for the scattering amplitude involving the potential term $1/|\vec{r}_1 - \vec{r}_2|$ is given by

$$g^B_{n'l',ns}\left(\frac{1}{|\vec{r}_1-\vec{r}_2|}\right) = i^{l'} 2\sqrt{\pi} 2^{l'} \Gamma(l'+2)\alpha_i\alpha_f \sum_j C(ns;j)\left(-\frac{\partial}{\partial\beta_i}\right)^{n_j-1} \sum_{j'} C(n'l';j')\left(-\frac{\partial}{\partial\beta_f}\right)^{n'_{j'}-1-l'} \beta_i \int_0^1 dy\, y(1-y)$$

$$\times \int_0^1 dz\, z\left(\frac{1}{\mu_1}\frac{\partial}{\partial\mu_1}\right)^2 \frac{1}{\mu_1}\left(\frac{1}{\mu_2}\frac{\partial}{\partial\mu_2}\right)\frac{1}{\mu_2}\frac{\lambda}{(\rho^2+\lambda^2)^{l'+2}}\rho^{l'} Y_{l'm'}(\hat{\rho}). \tag{A14}$$

Here, the expressions of μ_1, μ_2, ρ, and λ are as stated before.

[1] J. E. Blackwood, C. P. Campbell, M. T. McAlinden, and H. R. J. Walters, Phys. Rev. A **60**, 4454 (1999), and references therein.
[2] N. Zafar, G. Laricchia, M. Charlton, and A. Garner, Phys. Rev. Lett. **76**, 1595 (1992).
[3] A. J. Garner, G. Laricchia, and A. Ozen, J. Phys. B **29**, 5961 (1996).
[4] G. Laricchia, Hyperfine Interact. **100**, 71 (1996).
[5] A. J. Garner and G. Laricchia, Can. J. Phys. **74**, 518 (1996).
[6] M. T. McAlinden, F. G. R. S. MacDonald, and H. R. J. Walters, Can. J. Phys. **74**, 434 (1996).
[7] P. K. Sinha and A. S. Ghosh, Phys. Rev. A **58**, 242 (1998).
[8] H. S. W. Massey and C. B. O. Mohr, Proc. Phys. Soc. London **67**, 695 (1954).
[9] P. A. Fraser, Proc. Phys. Soc. London **78**, 329 (1961).
[10] S. Hara and P. A. Fraser, J. Phys. B **8**, L472 (1975).
[11] R. J. Drachman and S. K. Houston, Phys. Rev. A **12**, 885 (1975); *ibid.* **14**, 894 (1976).
[12] R. J. Drachman, Phys. Rev. A **19**, 1900 (1979).
[13] H. Ray and A. S. Ghosh, J. Phys. B **29**, 5505 (1996).
[14] H. Ray and A. S. Ghosh, J. Phys. B **30**, 3745 (1997).
[15] P. K. Sinha, P. Chaudhury, and A. S. Ghosh, J. Phys. B **30**, 4643 (1997).
[16] H. Ray and A. S. Ghosh, J. Phys. B **31**, 4427 (1998).
[17] C. P. Campbell, M. T. McAlinden, F. R. G. S. Mcdonald, and H. R. J. Walters, Phys. Rev. Lett. **80**, 5097 (1998).
[18] P. K. Biswas and S. K. Adhikari, J. Phys. B **31**, 3147 (1998).
[19] P. K. Sinha, A. Basu, and A. S. Ghosh, J. Phys. B **33**, 2579 (2000).
[20] R. J. Damburg and E. Karule, Proc. Phys. Soc. London **90**, 637 (1967).
[21] P. G. Burke and T. G. Webb, J. Phys. B **3**, L131 (1970).
[22] N. K. Sarkar, P. Chaudhury, and A. S. Ghosh, J. Phys. B **32**, 1657 (1999).
[23] P. K. Biswas and S. K. Adhikari, Phys. Rev. A **59**, 363 (1999).